The effect of media to reduce irradiation dose in crosslinking of self-assembled molecular layers

Ena Pezic[a], Helena Mijic[b], Branka Mihaljevic[a], Katarina Marusic[a,*]

[a] *Ruđer Bošković Institute, Division of Materials Chemistry, Bijenička cesta 54, Zagreb, Croatia*

[b] *University of Zagreb, Faculty of Chemical Engineering and Technology, Marulićev trg 19, Zagreb, Croatia*

* Corresponding author: kmarusic@irb.hr; kejt.marusic@gmail.com

Abstract

The present study aims to investigate the possibility of reducing the absorbed dose required to prepare a polymer nanocoating for surface functionalization by modifying the irradiation medium. We have studied the crosslinking of elaidic acid (EA), an unsaturated trans fatty acid, on oxidised copper by gamma irradiation. Three different irradiation media were compared: water purged with N_2, water purged with N_2O, and air purged with N_2. Contact angle measurements were used to determine the hydrophobicity of the surface. The coatings were investigated by electrochemical measurements: The degree of crosslinking was indirectly determined by polarisation measurements, while the behaviour of the coatings was studied by electrochemical impedance spectroscopy. The results showed that crosslinking can be achieved in all media studied. The highest dose of 110 kGy is required when irradiation is performed in oxygen-free air, while much lower doses of 40 kGy are required when irradiation is performed in water that has been purged with both gases used. The highest degree of crosslinking is achieved when irradiation is performed in air, while the degree of crosslinking when irradiated in water is highly dependent on the gas used. If N_2O is used, the degree of crosslinking is significantly higher. The surface of the coatings is more hydrophobic when polymer coatings are present on the surface, regardless of the irradiation medium.

Keywords: self-assembled molecular layers; radiation crosslinking; polymer nanocoatings; water radiolysis; irradiation in aqueous system; solid state irradiation.

1. Introduction

Self-assembled molecular layers (SAMs) are ordered molecular assemblies that can be formed spontaneously by chemisorption of organic molecules on a solid substrate surface (Ulman, 1996). Spontaneous adsorption occurs simply by exposing the substrate to a solution or gas containing the organic molecules with self-assembling properties (Ulman, 1991, 1996). Organic molecules forming such assemblies consist of three parts. The head group is responsible for chemisorption on the substrate and must have an appropriate affinity for the surface to which it binds. The alkyl chain joins the head group and gives the assembly an ordered and densely packed structure due to van der Waals forces between the chains. The third part is a terminal group that determines the new properties of the material. Many different organic molecules have been studied for the formation of SAMs on different metals. One of these molecules is alkanethiols, which can be adsorbed on a pure metal surface (Caipa Campos et al., 2011; Jennings & Laibinis, 1996), while molecules such as silanes (Franquet et al., 2003; Masi et al., 2019), phosphonic acids (Kruszewski et al., 2012; Wan et al., 2020; Cabrita et al., 2010; Kristan Mioč & Otmačić Ćurković, 2020; Raman et al., 2010), hydroxamic acids (Raman et al., 2010; Telegdi et al., 2007), or carboxylic acids (Kristan Mioč & Otmačić Ćurković, 2020; Raman et al., 2010; Marušić & Otmačić Ćurković, 2018; Tao, 1993; Hajdari et al., 2016; Jadhav, 2011; Marušić et al., 2014) bind to a metal oxide surface.

Fatty acids are carboxylic acids with long aliphatic chains that have the ability to self-assemble on metal surfaces. The carboxylate anion and the metal cation form a surface salt, which is the driving force for the spontaneous adsorption of fatty acids on the metal surface. The terminal -CH_3 group and the aliphatic chain are hydrophobic. Thus, when a fatty acid SAM is applied to the surface, the metal surface becomes hydrophobic and by repelling water from the surface, the metal becomes more stable and resistant to aggressive media (Ulman, 1996).

Despite many advantages, the main disadvantage for the widespread application of SAMs is their instability and ease of removal from the surface (Kaufmann et al., 2010). There are several studies on how to improve the durability of SAMs (Telegdi, 2020). One of the proposed solutions to improve the protective properties and stability of SAMs is their crosslinking. Crosslinking of SAMs leads to the formation of nanothick polymer coatings that are more stable and resistant to the penetration of external ions and molecules. Although many studies have been performed using classical crosslinking methods (Aramaki, 2007; Deng et al., 2008; Ghelichkhah et al., 2015), successful crosslinking using gamma irradiation has only recently been reported (Marušić et al., 2023). An important advantage of using ionizing radiation for crosslinking is that crosslinking can be performed in the solid state without using often toxic solvents or crosslinking agents.

In our previous work (Marušić et al., 2023), we have shown that SAMs formed from an unsaturated trans fatty acid, elaidic acid (EA), $C_{18}H_{34}O_2$, on copper can be successfully crosslinked in air without the presence of oxygen by gamma radiation at a dose of 110 kGy. The aim of this work was to investigate the possibility of reducing the absorbed dose required for successful crosslinking of SAMs by changing the irradiation medium, i.e. irradiating in water instead of air. The water medium used for irradiation was oxygen-free and was purged with N_2 and N_2O to compare the effects.

2. Materials and Methods

2.1. Sample preparation

Preparation of copper: The studies were carried out on samples of pure copper (high purity: 99.9%) cut into 0.5 cm thick pieces from a ⌀1.3 cm long rod. The specimens were abraded with 400, 800, 1500, and 2500 grit emery paper and polished with α-Al_2O_3 of 0.1 μm grit. They were cleaned under running tap water, rinsed with ethanol, and degreased with ethanol in an ultrasonic bath for 10 minutes. The samples were kept in a furnace at 80°C to form 24 hours for an oxide film on the surface.

Formation of the self-assembled molecular layer (SAM): Elaidic acid (EA), *trans*-octadec-9-enoic acid, $CH_3(CH_2)_7CH{=}CH(CH_2)_7COOH$, was purchased from Sigma-Aldrich Chemie GmbH and diluted in ethanol at a concentration of 10 mmol/L (EA solution). Copper samples were immersed in the EA solution for 24 hours at 40°C. The samples were rinsed extensively with ethanol to remove the excess of unbound EA molecules from the surface and then dried in a furnace at 50 °C for 24 hours. The EA SAM preparation procedure used was optimized in previous studies (Marušić et al., 2014).

Irradiation of specimens: The prepared samples were placed in glass flasks and irradiated in three different media: (1) Milli-Q water purged with N_2; (2) Milli-Q water purged with N_2O; and (3) air purged with N_2. Irradiation was performed in the ^{60}Co panoramic irradiation facility of the Radiation Chemistry and Dosimetry Laboratory, Division of Materials Chemistry, Ruđer Bošković Institute, at room temperature. The samples were irradiated with different doses ranging from 5 to 110 kGy at a dose rate of 22 kGy/h. The irradiation times were

calculated based on the dose map of the gamma source determined by the ECB dosimetry system and confirmed by computational simulations (Majer et al., 2019).

2.2. Characterization and analyses of copper samples

Electrochemical measurements were performed in a three-electrode cell using a PalmSens4 potentiostat/galvanostat/impedance analyzer. Samples were placed in corrosion cell holders designed to hold the rod-shaped samples. The surface of the specimens was exposed to the corrosion test solution with an area of 0.5 cm^2. A platinum foil was used as a counter electrode. A saturated calomel electrode (SCE) was used as the reference electrode, and all potentials in the text refer to the SCE scale. The corrosion test solution simulated atmospheric conditions and consisted of 0.2 g/L $NaHCO_3$ + 0.2 g/L $NaNO_3$ + 0.2 g/L Na_2SO_4 acidified to pH 5 with dilute H_2SO_4. The electrodes were immersed in the test solution for 45 minutes before measurements to stabilize the open circuit potential. Four measurements were made for each type of sample prepared in the same manner. *Polarization measurements* were performed with a wide potential range (±150mV OCP) and a potential scan rate of 0.166 mV/s.

Electrochemical impedance spectroscopy (EIS) was performed in the frequency range of 100 kHz–10 mHz at E_{corr} with an rms amplitude of 10 mV. Capacitive elements in real electrochemical systems are usually represented by the constant-phase element CPE due to frequency dispersion. The impedance of CPE is defined as $Z(\mathrm{CPE}) = \frac{1}{Q(j\omega)^n}$, where Q is the constant of the CPE element, j is the imaginary number, ω is the angular frequency, and n is the CPE exponent, where $-1 \leq n \leq 1$. The value of the pseudocapacitance C was calculated using the relation $C = \sqrt[n]{QR^{1-n}}$. Corrosion current densities were calculated using the Stern-Geary equation $j_{corr} = B/R_p$, where $B = \frac{b_a b_c}{2.303(b_a+b_c)}$ was calculated from the polarization measurement data.

Contact angles were measured on the samples using a DataPhysics Contact Angle System OCA 20 goniometer. Measurements were made using a 2 μL water droplet under atmospheric conditions. Six measurements were taken for each surface and a mean value was calculated.

3. Results and Discussion

In our previous work, we presented a method for crosslinking self-assembled molecular layers (SAMs) of elaidic acid (EA) in air in the absence of oxygen (Marušić et al., 2023). According to our studies, a dose of 110 kGy is required for successful crosslinking. In order to reduce the applied dose, we studied crosslinking in water in this work.

3.1. Irradiation in air

In the case of irradiation in solid state (in air), the radiation affects the material directly. In this case, the proposed crosslinking paths on EA SAM on copper are shown in Figure 1. This system was studied in our previous work where it is presented (Marušić et al., 2023).

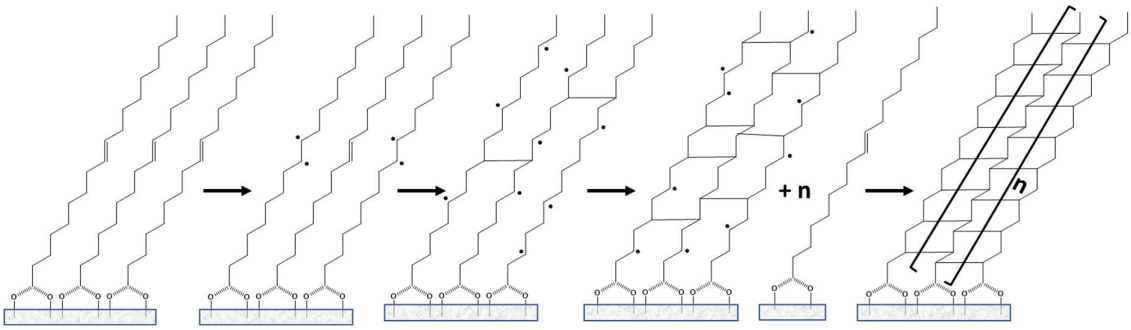

Figure 1. Simplified schematic representation of the radiolytic crosslinking of an EA SAM on a metal surface in the oxygen-free air system.

3.2. Irradiation in water

When a solid is irradiated in an aqueous system, the water makes up most of the system and receives a correspondingly large fraction of the absorbed energy. Accordingly, chemical changes occur in the solid as it reacts with the products of water radiolysis.

Water radiolysis consists of several stages (Spinks & Woods, 1990). The first stage, *the physical stage*, consists of energy deposition followed by rapid relaxation processes leading to the formation of ionized water molecules ($H_2O^{\bullet+}$), excited water molecules (H_2O^*), and prehydrated electrons (e^-):

$$H_2O \rightsquigarrow H_2O^{\bullet+}, e^- , H_2O^* \quad (1)$$

In the next stage, *the physicochemical stage*, several processes occur. The water radical cation $H_2O^{\bullet+}$ is a very strong acid and immediately loses a proton to water molecules forming hydroxyl radical:

$$H_2O^{\bullet+} + H_2O \rightarrow H_3O^+ + HO^{\bullet} \quad (2)$$

The excited water molecules (H_2O^*) undergo homolytic dissociation creating $H^{\bullet}$ and $OH^{\bullet}$ radicals:

$$H_2O^* \rightarrow HO^{\bullet} + H^{\bullet} \quad (3)$$

At the same time, the prehydrated electron undergoes hydration:

$$e^- + n\,H_2O \rightarrow e^-_{aq} \quad (4)$$

In the final stage, *the chemical stage*, the species react with each other and also with the surrounding molecules before diffusing into solution.

These three stages are summarized on the following equation:

$$H_2O \rightsquigarrow e^-_{aq} , HO^{\bullet}, H^{\bullet}, HO^{\bullet}_2, H_3O^+, OH^-, H_2O_2, H_2 \quad (5)$$

Radiolysis of neutral water leads to the formation of the dominant reactive products $^{\bullet}OH$, e_{aq}^-, and $H^{\bullet}$, with corresponding radiation chemical yields of $G(^{\bullet}OH)$ = 0.28 µmol J^{-1}, $G(e_{aq}^-)$ = 0.27 µmol J^{-1} and $G(H^{\bullet})$ = 0.062 µmol J^{-1} (Spinks & Woods, 1990).

The presence of oxygen and/or air during irradiation generates free radicals that are often rapidly converted to peroxide radicals. The fate of these radicals depends on the nature of the irradiated material, the potential scavengers present in the medium and parameters such as temperature, total dose, dose rate, etc. When fatty acids

are irradiated, it can be assumed that these radicals are involved in the degradation of the fatty acids before their crosslinking takes place.

3.2.1. Irradiation in water purged with N_2

Purging with N_2 is a standard procedure to physically displace oxygen from the system. In this part of the studies, oxygen was removed by purging water with N_2 prior to irradiation.

For the crosslinking of EA SAM, which covers the metal surface in water in the absence of oxygen, the proposed mechanism of radical polymerization is shown in Fig. 2. The primary radiolytic products formed after water irradiation ($H^{\bullet}$ and $OH^{\bullet}$) initiate the first reaction of radical addition on the double bond of the alkyl chain. After initiation, propagation reactions occur between the two neighbouring fatty acids. The reaction proceeds by the formation of reactive radicals centred on the carbon atom, $C^{\bullet}$. Although the reaction begins with the breaking of the double bonds of the EA molecules, further irradiation leads to the formation of additional reactive radicals on the carbon atom $C^{\bullet}$ by breaking the C-H bonds (Marušić et al., 2023), which serve as new crosslinking centres. The $OH^{\bullet}$ radical is the most important reactive species, because the $H^{\bullet}$ radicals recombine very rapidly to produce hydrogen gas, H_2.

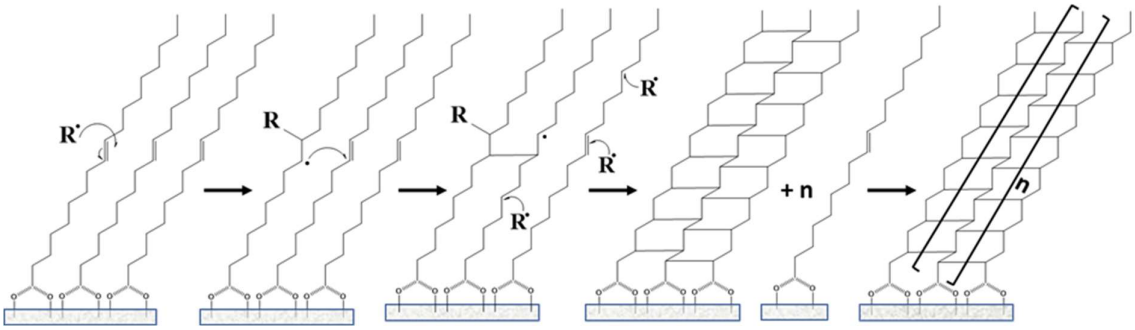

Figure 2. Simplified schematic presentation of radiolytic crosslinking of an EA SAM present on a metal surface in oxygen free aqueous system.

SAMs and the polymer nanocoatings (PNCs) obtained by their crosslinking are about 5 nm thick when prepared under the conditions used for this work (Marušić et al., 2023). It is difficult to study such thin coatings directly, so indirect methods are usually used. Since the stability of SAMs increases with crosslinking, it is possible to follow the progress of crosslinking by determining the corrosion current density in a corrosive medium: as the degree of crosslinking increases, the corrosion current density decreases. Simulated atmospheric conditions were used for these studies: 0.2 g/L $NaHCO_3$ + 0.2 g/L $NaNO_3$ + 0.2 g/L Na_2SO_4 (corrosion test solution).

Crosslinking of EA SAMs in water was investigated by polarization measurements in the corrosion test solution, and the corrosion parameters were determined from the obtained curves by the Tafel extrapolation method. The total current density (j) is the sum of anodic (j_a) and cathodic (j_c) current. For the potential region near the open circuit, both processes follow Tafel's law:

$$j = j_a + j_c = j_{corr}\,[\exp\{b_a(E - E_{corr})\} - \exp\{b_c(E - E_{corr})\}] \quad (6)$$

Corrosion parameters were evaluated against this equation using the nonlinear least squares method in a the potential range limited to ±70 mV with respect to E_{corr}.

Initially, a dose of 5 kGy was applied, which was then gradually increased while the corrosion current density and polarization resistance were determined. The results are shown in Figure 3.

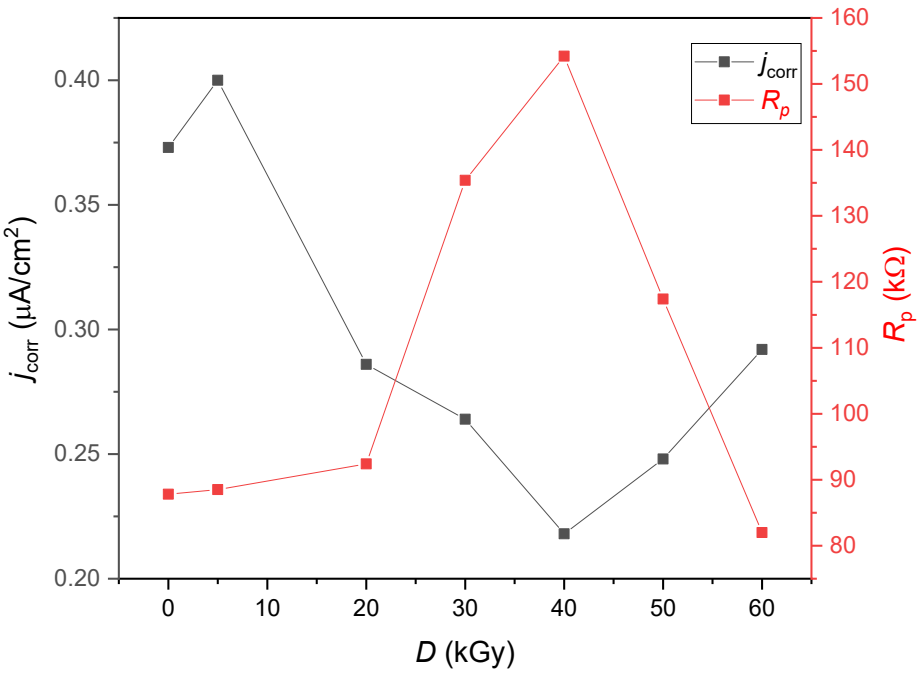

Figure 3. The corrosion current density and polarization resistance obtained by the Tafel extrapolation method from the polarization curves obtained in the corrosion test solution on copper samples covered by EA SAM irradiated in water purged with N_2.

It can be seen that no significant changes occurred at 5 kGy. However, at 20 kGy, a decrease in corrosion current density was observed, indicating that crosslinking had begun. When the dose was further increased, the corrosion current density continued to decrease until it reached the lowest measured value at 40 kGy. Further increase in irradiation dose resulted in higher corrosion current densities, indicating that the film was over-irradiated. Accordingly, the polarization resistance of the samples reached the highest value when irradiated with 40 kGy, 154.2 kΩ. It can be concluded that the dose of 40 kGy is the optimal irradiation dose for the crosslinking of SAMs in water without the presence of oxygen.

Table 1 shows all the corrosion parameters obtained from the polarization curves obtained by the Tafel extrapolation method on copper samples irradiated with EA SAM in water purged with N_2. It can be seen that the corrosion potential (E_{corr}) shifts slightly to higher potentials at the doses where the currents obtained are lowest.

Table 1. Corrosion parameters obtained by the Tafel extrapolation method in the corrosion test solution for non-irradiated SAM sample and samples of SAM irradiated in water purged with N_2.

D, kGy	b_a, mVdec^{-1}	$-b_c$, mVdec^{-1}	E_{corr}, mV$_{SCE}$	j_{corr}, µAcm^{-2}	R, kΩ	CD, %
0	41	256	-6	0.373 ± 0.063	87.8	-
5	46	221	-9	0.400 ± 0.158	88.5	-
20	47	213	-5	0.286 ± 0.136	92.4	23
30	44	183	4	0.264 ± 0.188	135.4	29
40	43	178	-1	0.218 ± 0.084	154.2	42
50	37	170	1	0.248 ± 0.088	117.4	34
60	30	210	-4	0.292 ± 0.114	82.0	22

Electrochemical impedance spectroscopy (EIS) was performed on the same type of samples. The scattered points in the graphs in Figure 4 show the results.

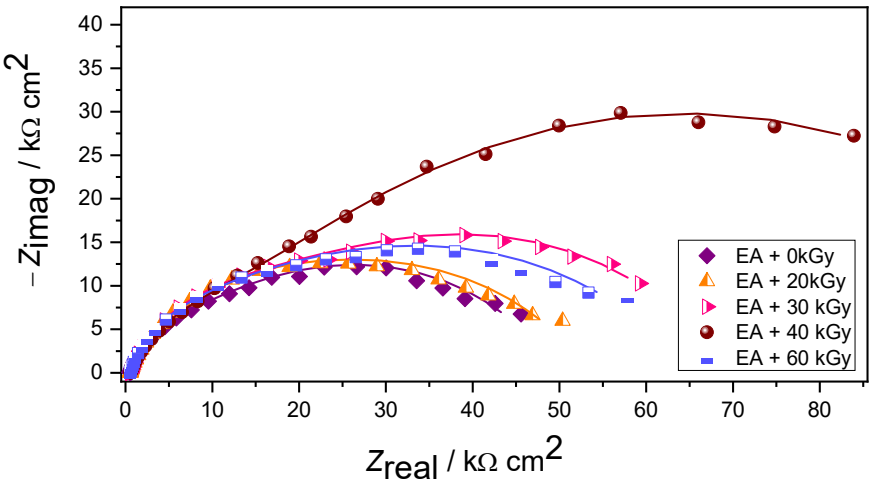

Figure 4. EIS results obtained in the corrosion test solution on samples of EA SAM applied to copper and irradiated to different doses in water purged with N_2 presented in Nyquist plot.

The size of the semicircle in the Nyquist diagram represents the total impedance of the system. The larger the semicircle, the greater the impedance, i.e., the resistance of the system to corrosion in the media to which it is exposed. It can be clearly seen that the impedance of the system increases at the doses shown in the figure. The largest increase is observed for the sample irradiated at 40 kGy, confirming that this is the optimal dose.

It should be noted that there is no way to measure the degree of crosslinking, but it is possible to estimate the degree by comparing the corrosion current densities of the coatings irradiated with different doses with those of the nonirradiated SAM according to the formula:

$$CD = \frac{j^0_{corr} - j^D_{corr}}{j^0_{corr}} \cdot 100\% \qquad (7)$$

where CD is the crosslinking efficiency (%), while j^0_{corr} and j^D_{corr} are the corrosion current densities (µAcm^{-2}) of the non-irradiated SAM and the polymer coatings obtained by irradiation with dose D (kGy). The results presented in Table 1 show that at the optimum irradiation dose of 40 kGy, the crosslinking degree is 42%.

When water is purged with N_2, oxygen is displaced from the system, thus avoiding peroxide radicals that may be involved in the degradation of fatty acids (Marušić et al., 2018). Although there are equivalent radiation chemical yields of $^{\bullet}OH$ and e_{aq}^- in our aqueous solutions, the reactions of hydroxyl radicals are expected to dominate over the reactions of hydrated electrons under the applied conditions. With a specific radical scavenger in the system, the formation of crosslinked coatings could be controlled by irradiation and directed to those that would exhibit better protective properties. To distinguish the involvement of electron and hydroxyl radical reactions and to confirm the dominant $^{\bullet}OH$ radical reactions, a common e_{aq}^- radical scavenger nitrogen(I)oxide, N_2O, was used.

3.2.2. Irradiation in water purged with N_2O

In N_2O-saturated solution (25 mM N_2O), irradiation converts e_{aq}^- to $^{\bullet}OH$ radicals, while $H^{\bullet}$ reacts slowly with N_2O ($k = 2.1 \times 10^6\ M^{-1}\ s^{-1}$) (Buxton et al., 1988; Spinks & Woods, 1990). The yields of reacting radicals $G(^{\bullet}OH)$ = 0.55 μmol J^{-1} and $G(H^{\bullet})$ = 0.062 μmol J^{-1} correspond to about 90 % of $^{\bullet}OH$ radicals and 10 % of $H^{\bullet}$ atoms (Buxton et al., 1988):

$$N_2O + e_{aq}^- \xrightarrow{H_2O} OH^{\bullet} + OH^- + N_2 \quad k = 9.1 \times 10^9\ M^{-1}\ s^{-1} \tag{8}$$

Thus, when N_2O is present in water during irradiation the amount of hydroxyl radicals is much higher than in water in equilibrium with air. In this way, the crosslinking process of the coating is further stimulated (Spinks & Woods, 1990).

The crosslinking of the EA SAMs obtained by irradiating their coatings in water saturated with N_2O was again studied by polarization measurements in the corrosion test solution, and from the obtained curves corrosion parameters were determined from the obtained curves using the Tafel extrapolation method. Crosslinking of the coatings in water saturated with N_2O was compared with irradiation under N_2 and with crosslinking in air purged with N_2. The results are summarized in Table 2.

Table 2. Corrosion parameters in the corrosion test solution for bare copper, unirradiated EA SAM (I) and samples irradiated with 40 kGy from SAM in aqueous media (II, III) and in air (IV) determined by the Tafel extrapolation method.

Sample	b_a, $mVdec^{-1}$	$-b_c$, $mVdec^{-1}$	E_{corr}, mV_{SCE}	j_{corr}, μAcm^{-2}	R_p, kΩ	***CD***, %	***η***, %
Bare Cu	44	164	-9	0.518 ± 0.015	58.0	-	-
I — SAM	41	256	-6	0.373 ± 0.063	87.8	-	28.0
II — 40, N_2, H_2O	43	178	-1	0.218 ± 0.084	154.2	41.6	57.9
III — 40, N_2O, H_2O	41	153	-1	0.154 ± 0.022	189.9	58.7	70.3
IV — 110, N_2, air	45	200	-7	0.136 ± 0.014	263.7	63.5	73.7

It can be seen from Table 2 that the corrosion current density is significantly lower for water purged with N_2O than for water purged with N_2. The determined value of 0.154 μAcm^{-2} is relatively close to the value of 0.136 μAcm^{-2} obtained for the samples irradiated in air. As for the crosslinking degree, the value of 58.7% obtained when irradiated in the presence of N_2O is relatively close to the value of 63.5 obtained for the samples irradiated in air.

In our previous work, where we studied the crosslinking in air (Marušić et al., 2023), we obtained higher values for the degree of crosslinking, namely over 90%, while the values for the corrosion current densities of the non-irradiated SAM were significantly higher. This difference is related to the different preparation methods used in the two studies. It is known that the preparation procedure significantly affects the properties of the SAM, so they can accordingly affect the properties of the crosslinked coatings. The main difference between the two studies is the drying step after self-assembling and before irradiation, which was significantly shorter than the procedure used in our previous work. According to literature (Marušić et al., 2014), the drying step is important for improving the protective properties of SAM. This was shown in our work, as the corrosion current densities of the SAM were lower with lower drying, but it seems to have a negative effect on the crosslinked SAM, where we obtained lower crosslinking degrees. Thus, the influence of the preparation process would be an interesting topic to investigate in the future.

The protective efficiency (η) of the different coatings can be calculated according to the following equation:

$$\eta = \frac{j_{Cu} - j_{Coat}}{j_{Coat}} \cdot 100\% \quad (9)$$

where j_{Cu} and j_{Coat} are the corrosion current densities measured on bare copper and on the differently coated samples. The results in Table 2 show that the samples irradiated in water in the presence of N_2O have an efficiency of 70.3% and the samples irradiated in air have an efficiency of 73.7 %. Compared to the 28.0 % obtained for the nonirradiated SAM, the improvement is quite significant.

The scattered points in Figure 5 show the results of the EIS measurements performed on the samples treated in different media and plotted in impedance diagrams. It can be clearly seen that the absolute impedance, i.e., resistance to electron flow at the interface, shown in Fig. 5a is highest for the samples irradiated in air and decreases when irradiated in water in the presence of N_2O, followed by the samples irradiated in water in the presence of N_2. These results confirm, the results of the polarization measurements.

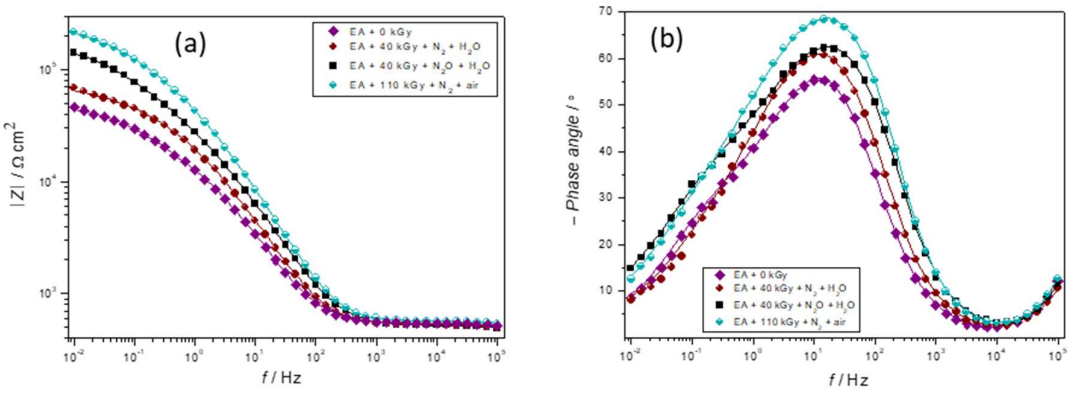

Figure 5. EIS data obtained on the compared coatings on copper in the test corrosion solution presented in Bode plots.

Although it is not always easy to extinguish, the experimental EIS data for all samples show two time constants under the capacitive loop. This means that the electrochemical process includes both the contribution of the double layer capacitance and the contribution of the coating on the copper surface. In the Bode diagram in Fig. 5b, it can be seen that all the curves have a maximum at frequencies around 10 Hz, with different values of the phase angles, which are shown in Table 3. This peak is related to the coatings covering the copper surface. An additional peak is observed in the low frequency range (around 0.1 Hz), which is due to the double layer. It can be seen that the maximum phase angles increase significantly after irradiation, indicating that the capacitive resistance in the system has increased.

Table 3. Phase angles obtained from the EIS results on the studied samples.

Sample	**I** — SAM	**II** — 40, N_2, H_2O	**III** — 40, N_2O, H_2O	**IV** — 110, N_2, air
Phase angle, °	55	61	62	69

The electrical equivalent circuit shown in Figure 6 was used for the regression calculation of the EIS data. The circuits consist of two *R*-*C* circuits in addition to the electrolyte resistance R_{el}. The value of the pseudocapacitance (*C*) was calculated as previously described (Marušić et al., 2018). The R_{ct}-C_{dl} circuit is related to the double layer capacitance and charge transfer resistance and is observed at low frequencies, as explained previously. The R_C-C_C circuit on the other hand is observed at high frequencies and is due to the influence of the coating on the corrosion reactions. The coefficients n_{ct} and n_f represent the depressed feature of the *R*-*C* circuits, respectively. Table 4 shows the results of the regression calculation.

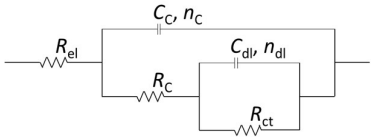

Figure 6. The equivalent electrical circuit used for fitting the obtained EIS data on the samples with the different coatings in simulated atmospheric conditions.

Table 4. Results of the regression calculation of the EIS data obtained on the different studied coatings using the equivalent electrical circuit presented in Fig. 5.

Sample	C_{dl}, μF cm^{-2}	n_{dl}	R_{ct}, kΩ cm^2	C_C, μF cm^{-2}	n_C	R_C, kΩ cm^2
I — SAM	5.8	0.84	12.5	44.3	0.60	36.8
II — 40, N_2, H_2O	4.6	0.85	21.6	28.3	0.52	52.3
III — 40, N_2O, H_2O	2.9	0.85	23.1	22.5	0.52	161.6
IV — 110, N_2, air	2.1	0.89	39.0	12.2	0.51	229.7

In all cases, both R_{ct} and R_C increased after irradiation. The III sample had virtually the same R_{ct} value as the II sample, but the value of R_C was significantly higher (161.6 versus 52.3 kΩ cm^2). The IV sample which was irradiated in air, showed even higher values for both R_{ct} (39.0 kΩ cm^2) and R_C (229.7 kΩ cm^2). In all cases, the capacitances showed the typical capacitive behaviour of the coatings, i.e., as the resistance increased, the capacitance decreased. In our previous work (Marušić et al., 2023), we showed that after irradiation, when the

coatings reach maximum crosslinking and are stable, C_{dl} is significantly lower compared to the unirradiated SAM, while in the cases where irradiation let to at least some degradation of the coatings, the values were similar or even higher than in the unirradiated SAM. This is due to the presence of reactive species on the copper surface, which are a consequence of the degradation of the coatings. Among the samples listed in Table 4, C_{dl} did not increase for any sample, but the value is relatively similar for the case of II sample (4.6 versus 5.8 μF cm^{-2}). The decrease is more pronounced for the other coatings. Crosslinking was achieved only at low levels, although it is clear that the coatings are no longer reactive.

The contact angle measurements were performed to investigate the hydrophobic properties of the surface of the coatings. Indeed, hydrophobicity plays an important role in the stability of the coatings, as it repels substances such as water, which contribute to the removal of the coatings from the surface. Table 5 shows the results obtained with the different coatings studied. It can be seen that the contact angles are significantly higher when the irradiated EA films are present on the surface. There is no significant difference between the values obtained for the different coatings, but they are all significantly higher than for bare copper. Considering that the value of 90° is considered the threshold value, it can be concluded that bare copper is hydrophilic, while the irradiated EA films make the surface hydrophobic.

Table 5. Contact angles of water drops with the different copper surfaces.

Sample	***Contact angle*, °**
I — SAM	49 ± 13
II — 40, N_2, H_2O	96 ± 7
III — 40, N_2O, H_2O	95 ± 12
IV — 110, N_2, air	97 ± 6

The results have shown that the optimal irradiation medium is air, while irradiation in water with N_2O is less effective to some extent, but is more convenient considering the price of irradiation. Nevertheless, it is not always convenient to perform irradiation in water. When irradiated in air, if the product is properly packaged, it is marketable and even sterile after irradiation, which is important for some applications. On the other hand, many products are not suitable to be kept in water for a long time (e.g., metallic items), and additional preparations must be made for the market. In summary, the choice of medium for irradiation should be evaluated and decided on a case-by-case basis.

The studies presented in this paper were performed on copper as the base metal. The behaviour of copper under atmospheric conditions is well known and therefore it is a convenient substrate to study the behaviour of the different layers on the surface. However, the process of self-assembly is similar for many metals, and therefore the fatty acids can be applied and crosslinked in the same way on the metals. Therefore, it is reasonable to assume that this type of coating can be applied to different metals.

The same is true for different fatty acids. This work was performed with an unsaturated fatty acid in the trans position. The results have shown that the double bond does not play a major role in the crosslinking of molecules, so it should be possible to crosslink different types of molecules, saturated and unsaturated. The trans position of the unsaturated molecules is important for the correct arrangement of the molecules on the surface, which is crucial

for successful crosslinking. The success of crosslinking depends strongly on the arrangement of the molecules. If the molecules are close enough and arranged in the correct order, crosslinking should occur, but this must be determined on a case-by-case basis.

4. Conclusions

Our study has shown that successful crosslinking of self-assembled molecular layers (SAMs) of elaidic acid (EA) on copper requires a dose of 110 kGy when irradiation is performed in oxygen-free air, as opposed to a dose of 40 kGy when irradiation is performed in oxygen-free water. The degree of crosslinking is highest for irradiation in air (64%), while irradiation in water depends on the gas used for purging. When N_2 is used to purge water, the degree of crosslinking is 42%, while in water saturated with N_2O it is much higher at 59%. All the coatings studied have shown a protective effect under simulated atmospheric conditions. When polymer nanocoatings are present on the surface, the copper surface becomes hydrophobic and the contact angle is 96° in all cases, regardless of the irradiation medium.

CRediT Authorship Contributions Statement

Conceptualization: K. Marusic, B. Mihaljevic; Data Curation: K. Marusic; Formal Analysis: E. Pezic, K. Marusic; Funding Acquisition: K. Marusic; Investigation: E. Pezic, H. Mijic; Methodology: K. Marusic; Project Administration: K. Marusic; Resources: K. Marusic; Software: E. Pezic; Supervision: K. Marusic; Validation: K. Marusic, B. Mihaljevic; Visualization: E. Pezic, K. Marusic, B. Mihaljevic; Writing – Original Draft Preparation: E. Pezic, K. Marusic; Writing – Review & Editing: K. Marusic.

Declaration of competing interest

The authors declare the following financial interests which may be considered as potential competing interests:

The financial support for the studies was provided by the Croatian Science Foundation.

Acknowledgements

The authors would like to thank the Croatian Science Foundation (HRZZ IP-2020-02-4344) for supporting this research.

References

Aramaki, K. (2007). Protection of zinc from corrosion by coverage with a hydrated cerium(III) oxide layer and ultrathin polymer films of a carboxylate self-assembled monolayer modified with alkyltriethoxysilanes. *Corrosion Science*, *49*(4), 1963–1980. https://doi.org/10.1016/j.corsci.2006.07.008

Buxton, G. V., Greenstock, C. L., Helman, W. P., & Ross, A. B. (1988). Critical Review of rate constants for reactions of hydrated electrons, hydrogen atoms and hydroxyl radicals (·OH/·O− in Aqueous Solution. *Journal of Physical and Chemical Reference Data*, *17*(2), 513–886. https://doi.org/10.1063/1.555805

Cabrita, J. F., Viana, Ana. S., & Abrantes, L. M. (2010). Copper Protection by Phosphonic Acid Self-assembled Monolayers. *Corrosion Protection of Materials*, *29*(4), 114–119.

Caipa Campos, M. A., Trilling, A. K., Yang, M., Giesbers, M., Beekwilder, J., Paulusse, J. M. J., & Zuilhof, H. (2011). Self-Assembled Functional Organic Monolayers on Oxide-Free Copper. *Langmuir*, *27*(13), 8126–8133. https://doi.org/10.1021/la200932w

Deng, H., Nanjo, H., Qian, P., Xia, Z., Ishikawa, I., & Suzuki, T. M. (2008). Corrosion prevention of iron with novel organic inhibitor of hydroxamic acid and UV irradiation. *Electrochimica Acta*, *53*(6), 2972–2983. https://doi.org/10.1016/j.electacta.2007.11.008

Franquet, A., Le Pen, C., Terryn, H., & Vereecken, J. (2003). Effect of bath concentration and curing time on the structure of non-functional thin organosilane layers on aluminium. *Electrochimica Acta*, *48*(9), 1245–1255. https://doi.org/10.1016/S0013-4686(02)00832-0

Ghelichkhah, Z., Sharifi-Asl, S., Farhadi, K., Banisaied, S., Ahmadi, S., & Macdonald, D. D. (2015). L-cysteine/polydopamine nanoparticle-coatings for copper corrosion protection. *Corrosion Science*, *91*, 129–139. https://doi.org/10.1016/j.corsci.2014.11.011

Hajdari, Z., Ćurković, H. O., Čadež, V., & Šegota, S. (2016). Corrosion Protection of Cupronickel Alloy by Self-Assembled Films of Fatty Acids. *Journal of The Electrochemical Society*, *163*(5), C145–C155. https://doi.org/10.1149/2.0321605jes

Jadhav, S. (2011). Self-assembled monolayers (SAMs) of carboxylic acids: an overview. *Open Chemistry*, *9*(3), 369–378. https://doi.org/10.2478/s11532-011-0024-8

Jennings, G. K., & Laibinis, P. E. (1996). Self-assembled monolayers of alkanethiols on copper provide corrosion resistance in aqueous environments. *Colloids and Surfaces A: Physicochemical and Engineering Aspects*, *116*(1–2), 105–114. https://doi.org/10.1016/0927-7757(96)03626-6

Kaufmann, C. R., Mani, G., Marton, D., Johnson, D. M., & Agrawal, C. M. (2010). Long-term stability of self-assembled monolayers on 316L stainless steel. *Biomedical Materials*, *5*(2), 025008. https://doi.org/10.1088/1748-6041/5/2/025008

Kristan Mioč, E., & Otmačić Ćurković, H. (2020). Protective films of stearic and octadecylphosphonic acid formed by spray coating. *Journal of Electrochemical Science and Engineering*, *10*(2), 161–175. https://doi.org/10.5599/jese.739

Kruszewski, K. M., Renk, E. R., & Gawalt, E. S. (2012). Self-assembly of organic acid molecules on the metal oxide surface of a cupronickel alloy. *Thin Solid Films*, *520*(13), 4326–4331. https://doi.org/10.1016/j.tsf.2012.02.064

Majer, M., Roguljić, M., Knežević, Ž., Starodumov, A., Ferenček, D., Brigljević, V., & Mihaljević, B. (2019). Dose mapping of the panoramic 60Co gamma irradiation facility at the Ruđer Bošković Institute – Geant4 simulation and measurements. *Applied Radiation and Isotopes*, *154*. https://doi.org/10.1016/j.apradiso.2019.108824

Marušić, K., Hajdari, Z., & Čurković, O. (2014). Optimizing the preparation procedure of self-Assembled monolayer of stearic acid for protection of cupronickel alloy. *Acta Chimica Slovenica*, *61*(2).

Marušić, K., Matijaković, N., & Mihaljević, B. (2018). Influence of Gamma Irradiation on a Fatty Acid Self-Assembling Coating of Copper. *Journal of The Electrochemical Society*, *165*(16), C973–C979. https://doi.org/10.1149/2.1301814jes

Marušić, K., & Otmačić Ćurković, H. (2018). Self-Assembling Monolayers of Stearic Acid in Protection of Steel. *Croatica Chemica Acta*, *91*(4). https://doi.org/10.5562/cca3436

Marušić, K., Pezić, E., Matijaković Mlinarić, N., Dubček, P., Sancho-Parramon, J., Kralj, D., & Mihaljević, B. (2023). Green Nanocoatings Prepared by Crosslinking Self-Assembled Fatty Acids on Metals. *Small*. https://doi.org/10.1002/smll.202301104

Masi, G., Josse, C., Esvan, J., Chiavari, C., Bernardi, E., Martini, C., Bignozzi, M. C., Monticelli, C., Zanotto, F., Balbo, A., Svara Fabjan, E., Kosec, T., & Robbiola, L. (2019). Evaluation of the protectiveness of an organosilane coating on patinated Cu-Si-Mn bronze for contemporary art. *Progress in Organic Coatings*, *127*, 286–299. https://doi.org/10.1016/j.porgcoat.2018.11.027

Raman, A., Quiñones, R., Barriger, L., Eastman, R., Parsi, A., & Gawalt, E. S. (2010). Understanding Organic Film Behavior on Alloy and Metal Oxides. *Langmuir*, *26*(3), 1747–1754. https://doi.org/10.1021/la904120s

Spinks, J. W. T., & Woods, R. J. (1990). Water and inorganic aqueous systems. In *Introduction to Radiation Chemistry* (Third, pp. 243–313). Wiley.

Tao, Y.-T. (1993). Structural Comparison of Self-Assembled Monolayers of n-Alkanoic Acids on the Surfaces of Silver, Copper, and Aluminum. *Journal of the American Chemical Society*, *115*(10), 4350–4358.

Telegdi, J. (2020). Formation of Self-Assembled Anticorrosion Films on Different Metals. *Materials*, *13*(22), 5089. https://doi.org/10.3390/ma13225089

Telegdi, J., Otmačić-Ćurković, H., Marušić, K., Al-Taher, F., Stupnišec-Lisac, E., & Kálmán, E. (2007). Inhibition of copper corrosion by self assembled amphiphiles. *Chemical and Biochemical Engineering Quarterly*, *21*(1).

Ulman, A. (1991). *An Introduction to Ultrathin Organic Films*. Elsevier. https://doi.org/10.1016/C2009-0-22306-3

Ulman, A. (1996). Formation and Structure of Self-Assembled Monolayers. *Chemical Reviews*, *96*(4), 1533–1554. https://doi.org/10.1021/cr9502357

Wan, X., Lieberman, I., Asyuda, A., Resch, S., Seim, H., Kirsch, P., & Zharnikov, M. (2020). Thermal Stability of Phosphonic Acid Self-Assembled Monolayers on Alumina Substrates. *The Journal of Physical Chemistry C*, *124*(4), 2531–2542. https://doi.org/10.1021/acs.jpcc.9b10628